

LETTERS

Nitrate supply from deep to near-surface waters of the North Pacific subtropical gyre

Kenneth S. Johnson¹, Stephen C. Riser² & David M. Karl³

Concentrations of dissolved inorganic carbon (DIC) decrease in the surface mixed layers during spring and summer in most of the oligotrophic ocean. Mass balance calculations require that the missing DIC is converted into particulate carbon by photosynthesis^{1–3}. This DIC uptake represents one of the largest components of net community production in the world ocean^{2,4}. However, mixed-layer waters in these regions of the ocean typically contain negligible concentrations of plant nutrients such as nitrate and phosphate^{3,5}. Combined nutrient supply mechanisms including nitrogen fixation, diffusive transport and vertical entrainment are believed to be insufficient to supply the required nutrients for photosynthesis^{6,7}. The basin-scale potential for episodic nutrient transport by eddy events is unresolved^{8,9}. As a result, it is not understood how biologically mediated DIC uptake can be supported in the absence of nutrients. Here we report on high-resolution measurements of nitrate (NO_3^-) and oxygen (O_2) concentration made over 21 months using a profiling float deployed near the Hawaii Ocean Time-series station in the North Pacific subtropical gyre. Our measurements demonstrate that as O_2 was produced and DIC was consumed over two annual cycles, a corresponding seasonal deficit in dissolved NO_3^- appeared in water at depths from 100 to 250 m. The deep-water deficit in NO_3^- was in near-stoichiometric balance with the fixed nitrogen exported to depth. Thus, when the water column from the surface to 250 m is considered as a whole, there is near equivalence between nutrient supply and demand. Short-lived transport events (<10 days) that connect deep stocks of nitrate to nutrient-poor surface waters were clearly present in 12 of the 127 vertical profiles.

Seasonal depletion of DIC in the surface mixed layer with insufficient concentrations or fluxes of inorganic fixed nitrogen (NO_3^- , NO_2^- and NH_4^+) present to support plant growth was first observed at the Bermuda Atlantic Time-series Study station¹. DIC also decreases through late winter to early autumn at the Hawaii Ocean Time-series (HOT) station (Fig. 1a), and this depletion results primarily from biological uptake¹⁰. Net community production (NCP) rates derived from the seasonal DIC cycle ($2.3 \pm 0.8 \text{ mol m}^{-2} \text{ yr}^{-1}$)¹⁰ in the mixed layer (upper 50–90 m) would require an annual nitrate concentration drawdown of $\sim 4 \mu\text{mol l}^{-1}$ at a nominal molar ratio for C/N of 6.6, which is greatly in excess of observed mixed-layer nitrate (Fig. 1b). An alternative estimate of the inorganic fixed nitrogen requirement comes from the particulate organic nitrogen export observed at 150 m at the HOT station^{11,12}, which averages $105 \text{ mmol N m}^{-2} \text{ yr}^{-1}$ (Table 1). There is also an organic nitrogen loss, associated with zooplankton migration¹², of $38 \text{ mmol N m}^{-2} \text{ yr}^{-1}$, for a total export of $143 \text{ mmol N m}^{-2} \text{ yr}^{-1}$ (Table 1). The mean nitrate gradient ($79 \mu\text{mol m}^{-4}$)¹³ is at least five times too low to supply the needed flux if the eddy diffusion coefficient is near $0.1 \text{ cm}^2 \text{ s}^{-1}$, as observed in tracer release experiments¹⁴. Furthermore, the nitrate gradient is near

zero at 100 m, which is well below the primary production maximum in the mixed layer (Fig. 1d). Dissolved organic nitrogen shows no concentration decrease comparable to the nitrogen requirement ($\sim 4 \mu\text{mol l}^{-1}$) through the year (Fig. 1c) and does not seem to be a source for the missing nitrogen³. Direct measurements of nitrogen fixation rates at the HOT station account for only 40% of the export nitrogen flux^{11,15} (Table 1). Understanding the mechanisms that supply nutrients to the shallowest layer of the ocean, where most NCP occurs, is critical to developing a capability to predict the response of ocean ecosystems to a changing climate¹⁶.

We have examined the annual cycle of nitrate and dissolved oxygen concentrations using chemical sensors on a profiling float deployed near the HOT station in the North Pacific subtropical gyre (Methods Summary). Seawater density, dissolved oxygen anomaly ($\text{O}_{2\text{Anom}} = \text{O}_2 - \text{O}_{2,100\% \text{Saturation}}$), nitrate and preformed nitrate (PreNO_3^-) observed in the upper 300 m of the water column are shown in Fig. 2. Preformed nitrate approximates the amount of nitrate present

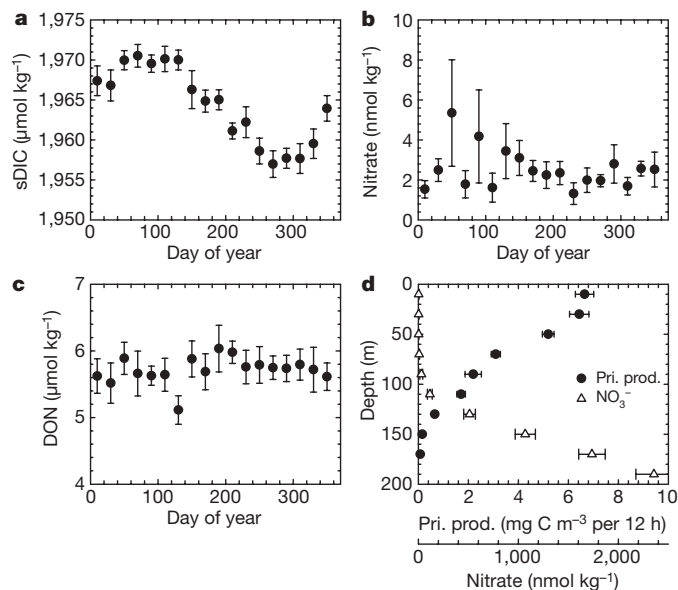


Figure 1 | Shipboard observations at HOT station ALOHA. **a**, DIC concentration normalized to salinity 35 in the upper 50 m versus day of year. A linear trend due to increasing atmospheric CO_2 , noted previously¹⁰, was removed from the data. **b**, Nitrate concentration in the upper 50 m measured by chemiluminescence versus day of year. **c**, Dissolved organic nitrogen versus day of year. **d**, Primary production measured with ^{14}C and nitrate versus depth. Data from 1988 to 2007 were downloaded from the HOT Data Organization & Graphical System website (<http://hahana.soest.hawaii.edu/hot/hot-dogs/interface.html>). Results were binned in 20-d or 20-m intervals and the mean and 95% confidence interval were computed.

¹Monterey Bay Aquarium Research Institute, Moss Landing, California 95039, USA. ²School of Oceanography, University of Washington, Seattle, Washington 98195, USA. ³School of Ocean and Earth Science and Technology, Center for Microbial Oceanography: Research and Education, University of Hawaii, Honolulu, Hawaii 96822, USA.

Table 1 | Organic and inorganic fixed nitrogen flux summary

| Process | Flux \pm 95% CI ($\text{mmol m}^{-2} \text{yr}^{-1}$) | Reference |
|---|---|-----------|
| NCP N requirement* | 287 ± 100 | 10 |
| Particulate organic N export at 150 m | 105 ± 7 | 12 |
| Zooplankton organic N export | 38 ± 4 | 12 |
| Total organic N loss | 143 ± 11 | — |
| Nitrogen fixation† | 41 ± 8 | 15 |
| Integrated NO_3^- deficit‡ | 160 ± 78 | This work |
| Integrated PreNO_3^- deficit‡ | 103 ± 39 | This work |
| Total inorganic N supply | 144 ± 47 to 201 ± 86 | — |
| HOT integrated NO_3^- deficit§ | 94 ± 66 | This work |
| Event-driven vertical NO_3^- transport | >88 | This work |

CI, confidence interval.

* Computed from the reported NCP value and a C/N ratio of 8.0.

† Integrated from 0 to 100 m.

‡ Integrated from 100 to 250 m. The deficit was calculated as values in months December to February minus values in months June to August.

§ Winter-to-summer difference of integrated (100–200 m) nitrate using HOT cruise data from 2000 to 2008 with more than eight nitrate measurements in the integral region. The integral was not extended to 250 m because vertical resolution is often near 50 m below 200 m and rapidly increasing nitrate combined with poor depth resolution skews the result.

|| Calculated as $>145 \text{ mmol m}^{-2} \times (365 \text{ d}/600 \text{ d}) \text{ yr}^{-1}$.

in a water mass when it leaves the ocean surface¹⁷. It was computed as $\text{PreNO}_3^- = \text{NO}_3^- - \text{O}_{2\text{Anom}}/R_{\text{O}_2/\text{NO}_3}$, where $R_{\text{O}_2/\text{NO}_3} = -10.5$ is the modified Redfield ratio¹⁸ of oxygen production to nitrate uptake. PreNO_3^- concentrations are near zero in surface waters at the HOT station, and values increase to 4–5 $\mu\text{mol l}^{-1}$ at a depth of 300 m. There is an anomalous layer of water¹⁷ with negative PreNO_3^- concentrations below the depth of the 1% light level (~ 115 m) that is well defined in our data (Fig. 2d). Negative PreNO_3^- below the mixed layer results if nitrate is assimilated into biomass and a corresponding amount of oxygen is not produced, or if oxygen is consumed and nitrate is not produced. Reasonable changes in $R_{\text{O}_2/\text{NO}_3}$ do not eliminate the negative PreNO_3^- values^{17,19}. We use PreNO_3^- in our analysis because it has a smaller dynamic range than nitrate, which makes the concentration decrease easier to visualize (Fig. 2d). However, all of the conclusions discussed below are similar regardless of whether NO_3^- or PreNO_3^- concentration is used.

Seasonal decreases occurred in depth-integrated (100–250 m) NO_3^- and PreNO_3^- (Fig. 2d and Supplementary Fig. 4). The decreases

in NO_3^- and PreNO_3^- were strongly related to an increase in oxygen anomaly at lesser depths (integrated from 50 to 100 m; Supplementary Fig. 4) that resulted from positive NCP²⁰. The winter-to-summer decrease in PreNO_3^- below the euphotic zone was driven primarily by a nitrate concentration decrease. Nitrate depletion at the base of the euphotic zone near the HOT station has been observed during summer and attributed to a 30-m downward displacement in isolines in summer²¹. However, the depletion in nitrate occurs down to a depth of 250 m (Fig. 2c, d), and additional processes must be involved.

Depth-integrated $\text{O}_{2\text{Anom}}$ below the mixed layer, but in the euphotic zone (50–100 m), and depth-integrated PreNO_3^- in deeper waters (100–250 m) were negatively correlated (coefficient of correlation, $R = -0.57$, $P < 0.001$) with the largest depletions in PreNO_3^- occurring in late summer (Fig. 2d and Supplementary Fig. 4). This is consistent with NO_3^- uptake at depth supporting NCP nearer the surface. The annual decrease in integrated PreNO_3^- was $103 \pm 39 \text{ mmol N m}^{-2}$ (95% confidence interval), using data from both years (Table 1). If depth-integrated nitrate concentration is used, then the decrease is $160 \pm 78 \text{ mmol N m}^{-2}$ (95% confidence interval). The second value is an upper bound on nitrate loss, as some of it is compensated for by an increase in $\text{O}_{2\text{Anom}}$ at depth. The sum of the PreNO_3^- decrease and the observed nitrogen fixation rate at the HOT station¹⁵ brackets the loss of organic nitrogen driven by particle flux and zooplankton migration (Table 1). Nitrate measurements made at the HOT station show a similar seasonal trend when data from 2000 to 2008 are binned, although the results are sensitive to the analysis method, perhaps because of the lower spatial and temporal resolution (Table 1).

Although the combined inorganic fixed nitrogen supplies are similar to organic nitrogen losses, they are somewhat less than the amount of nitrogen required to support observed NCP ($287 \pm 100 \text{ mmol N m}^{-2} \text{yr}^{-1}$; Table 1) at a C/N ratio of 8.0, which is observed in sinking particles near the HOT station^{12,22}. Primary production, organic nitrogen export and C/N all show significant interannual variability near the HOT station¹², which may account for this discrepancy. The slope of depth-integrated $\text{O}_{2\text{Anom}}$ versus PreNO_3^- in the float data set is $-2.8 \pm 0.4 \text{ mol O}_2$ per mol N (Supplementary Fig. 4b). Because only $25 \pm 10\%$ of the oxygen created by NCP is trapped beneath the thermocline near the HOT station^{10,20,23},

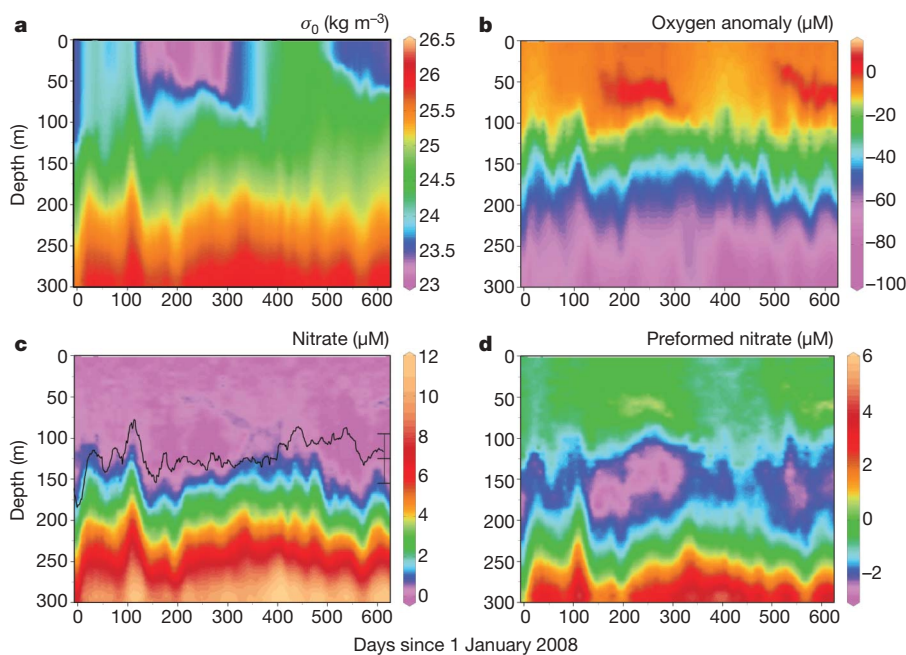


Figure 2 | Profiling float observations in the upper 300 m. Measurements were made at 5-d intervals and with 5-m vertical resolution above 100 m and 10-m resolution below. **a**, Seawater density anomaly ($\sigma_0 = \text{density} - 1,000 \text{ kg m}^{-3}$). **b**, Oxygen anomaly ($\text{O}_2 - \text{O}_{2,100\% \text{Saturation}}$). **c**, Nitrate. The black line shows sea surface height anomaly (SSHA; <http://www.avisioceanobs.com/duacs/>) at the location of each float profile. The SSHA scale bar is centred on zero and spans -10 cm (top) to 10 cm (bottom). **d**, Preformed nitrate. Data contoured using Ocean Data View 3.4 (Schlitzer, R., <http://odv.awi.de>).

www.avisioceanobs.com/duacs/) at the location of each float profile. The SSHA scale bar is centred on zero and spans -10 cm (top) to 10 cm (bottom). **d**, Preformed nitrate. Data contoured using Ocean Data View 3.4 (Schlitzer, R., <http://odv.awi.de>).

the ratio of NCP to the change in PreNO_3^- in water sampled by the float was -11 ± 6 mol O_2 per mol N. This is consistent with the modified Redfield ratio¹⁸ of -10.5 . The consistency implies lower-than-average NCP during the observing period. In any case, the float data set resolves a previously unidentified nitrate source that is much larger than other recognized inorganic fixed nitrogen sources.

Episodic transport events are often suggested to be the mechanisms responsible for supplying deep, nutrient-rich water to the euphotic zone^{7,8,24}. The profiling float data clearly showed episodic entrainment of nitrate into the euphotic zone. Nitrate concentrations reached $1 \mu\text{M}$ at a depth of 80 m in the euphotic zone in one such event (9 February 2009), which is labelled 2 in Fig. 3. Isopycnals were uplifted in this event, but enhanced mixing also drove nitrate across isopycnals to reach lesser depths (Fig. 3b). This profile was collected on the boundary of a low feature in sea surface topography that forms closed contours, similar to a cyclonic eddy (Fig. 3d). The high nitrate concentration was confirmed by the simultaneous signals in oxygen and salinity (Fig. 3), which are measured by independent sensors. Such events have a short lifetime (less than twice the float cycle time) or are spatially variable, and the observations do not resolve the fate of the uplifted nitrate. Another event (labelled 1 in Fig. 3), which occurred three weeks earlier than event 2, also showed a salinity anomaly penetrating into the euphotic zone, but the nitrate near the top of this event seemed to be missing and consumed by phytoplankton.

The profiling float data set is unique in that it allows a systematic, model-independent assessment of the probability of nutrient transport episodes, magnitudes and their vertical extent. The probability of events through the whole data set (12 events with evidence of $1 \mu\text{M}$ nitrate above 110 m in 127 float cycles) is about that shown in Fig. 3 (2 such events in 19 float cycles). It is also similar to the probability of high nutrient events seen at the HOT station (12 of 135 cruises; see fig. 16.7b of ref. 25). Event 2 (Fig. 3) showed the highest penetration of nitrate into the euphotic zone. Vertical integration of the observed

nitrate anomalies that extended above 110 m, near the 1% light level, and the nitrate anomalies that might have been present, assuming a conservative relationship with salinity, summed to $145 \text{ mmol N m}^{-2}$ over 600 days. The integral sum is a minimum estimate. We did not count events with less than $1 \mu\text{M}$ (for example the event marked 3? in Fig. 3b). Furthermore, if events occurred at a higher frequency than half the float profile frequency, then the number of events would be undercounted and the integral would be still higher.

If all nitrate transported above 110 m were consumed, as seems to be the case in several events where salinity anomalies are present with no nitrate, then the events observed by the float transported at least $88 \text{ mmol N m}^{-2} \text{ yr}^{-1}$ up to depths of 75 m in the euphotic zone. This is in near balance with the amount of PreNO_3^- that disappeared between 100 and 250 m, and the sum of episodic nitrate transport and the nitrogen fixation rate nearly equals organic nitrogen loss rates (Table 1). However, the bulk of NCP occurs in the mixed layer¹⁰, which is typically shallower than the depths reached by nitrate injection events. Additional processes must be involved to allow the nitrate to reach the zone where most NCP occurs. Furthermore, to produce the DIC drawdown observed in the mixed layer¹⁰, vertical nitrate transport over the last few tens of metres into the mixed layer must occur without simultaneous transport of DIC. This rules out any direct physical transport mechanism, because water that carries elevated nitrate will also transport elevated DIC and that would eliminate surface DIC drawdown.

Twenty per cent of the integrated stock of chlorophyll at the HOT station is found between 125 and 200 m, which is well below the chlorophyll maximum at 100 m (Supplementary Fig. 5). Although the fraction of phytoplankton biomass below 125 m is less than 20% of the total due to photo-adaptation, these data clearly show the continuous presence of phytoplankton deep in the water column. We suggest that the phytoplankton present in the deep waters must be able to consume the nitrate that is transported vertically in these events. The

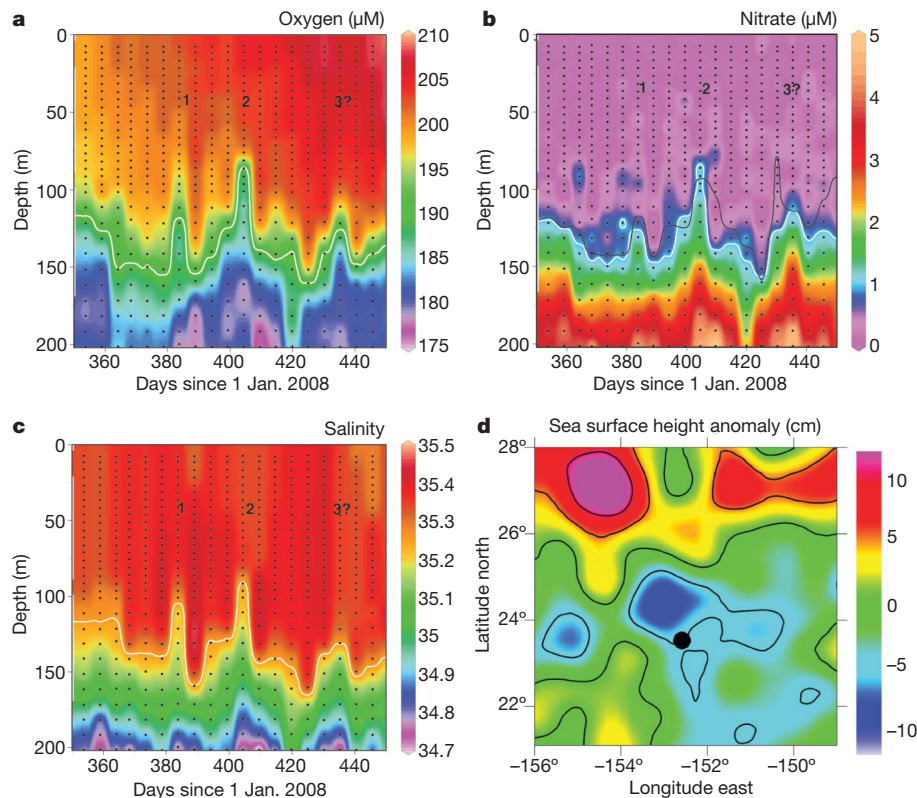


Figure 3 | Profiling float observations over 100 days from 19 December 2008 to 22 March 2009. **a**, Dissolved oxygen. Black dots show the location of each measurement. White line is the $190 \mu\text{M}$ contour. Vertical transport events discussed in the text are identified using the labels 1, 2 and 3?.

b, Nitrate. White line is the $1 \mu\text{M}$ contour. Black line is the 24.55 kg m^{-3} density anomaly contour. **c**, Salinity. White line is the 35.25 contour. **d**, Sea surface height anomaly on 11 February 2009 (407 days after 1 January 2008). The black dot shows the profile location during event 2.

phytoplankton must then detrain from the upwelled plumes by upward motility, perhaps through buoyancy regulation, before the water returns to depth. Upward transport of 6–35 mmol N m⁻² yr⁻¹ by phytoplankton has been estimated from observations of relatively rare mats of large diatoms²⁶. That work focused on large phytoplankton aggregates because of their capability for long vertical migrations. The frequent vertical motions observed by the profiling float and their vertical scope suggest that simpler mechanisms involving smaller-scale migrations, for example by individual phytoplankton, may support the remainder of the upward transport.

Our observations suggest that episodes of vertical nutrient transport, at frequencies near monthly, are a major factor sustaining positive NCP in the North Pacific subtropical gyre. In combination with our previous results²⁰, which show little or no episodicity in oxygen production, this suggests that near-monthly inputs of nutrients must be sufficient to sustain positive NCP during the intervening periods.

METHODS SUMMARY

Float 5145 (WMO #5901468) is a Webb Research APEX profiling float that was fabricated at the University of Washington and the Monterey Bay Aquarium Research Institute with an integral *in situ* ultraviolet spectrophotometer (ISUS) nitrate sensor²⁷ that uses an improved algorithm²⁸ and an Aanderaa Optode dissolved-oxygen sensor²⁹. The float cycled from 1,000-m depth to the surface every five days, beginning in December 2007, as it drifted east (Supplementary Fig. 1). Nitrate and oxygen measurements were made at 60 depths (5-m resolution above 100 m, 10-m resolution from 100 to 360 m and 50-m resolution from 400 to 1,000 m) during the ascent.

The optical absorption baseline in ISUS underwent two jumps (Supplementary Fig. 2a). These shifts offset the entire nitrate profile from 1,000 m to the surface by about 1 μM (Supplementary Fig. 2b). To remove these offsets, we have assumed that nitrate concentration in the upper 30 m of the water column was 0.0025 μmol l⁻¹, which is equal to the mean of the long-term HOT data record (Fig. 1b). The mean nitrate concentration that was reported by the float nitrate sensor in the upper 30 m of each profile was then subtracted from each individual measurement on that profile. The resulting data set has a precision (1 s.d. of corrected nitrate concentrations on 125 profiles) of 0.3 μmol l⁻¹ (Supplementary Fig. 2) and it is in excellent agreement with the mean HOT nitrate profiles reported for 2007 to 2008 (Supplementary Fig. 3). The oxygen sensor shows no evidence of drift, but it seems to have a small accuracy bias (<10 μmol l⁻¹), as reported for earlier applications of Aanderaa Optode sensors on profiling floats³⁰ (Supplementary Fig. 3).

Received 6 October 2009; accepted 29 April 2010.

1. Michaels, A. F., Bates, N. R., Buesseler, K. O., Carlson, C. A. & Knap, A. H. Carbon-cycle imbalances in the Sargasso Sea. *Nature* **372**, 537–540 (1994).
2. Lee, K. Global net community production estimated from the annual cycle of surface water total dissolved inorganic carbon. *Limnol. Oceanogr.* **46**, 1287–1297 (2001).
3. Karl, D. M. *et al.* in *Ocean Biogeochemistry* (ed. Fasham, M. J. R.) 239–267 (Springer, 2003).
4. Emerson, S. *et al.* Experimental determination of the organic carbon flux from open-ocean surface waters. *Nature* **389**, 951–954 (1997).
5. Karl, D. M. & Letelier, R. M. Nitrogen fixation-enhanced carbon sequestration in low nitrate, low chlorophyll seascapes. *Mar. Ecol. Prog. Ser.* **364**, 257–268 (2008).
6. Williams, R. G. & Follows, M. J. in *Ocean Biogeochemistry* (ed. Fasham, M. J. R.) 19–51 (Springer, 2003).
7. Jenkins, W. J. & Doney, S. C. The subtropical nutrient spiral. *Glob. Biogeochem. Cycles* **17**, 1110 (2003).
8. McGillicuddy, D. J. Jr *et al.* Eddy/wind interactions stimulate extraordinary midocean plankton blooms. *Science* **316**, 1021–1026 (2007).
9. Martin, A. P. & Pondaven, P. On estimates for the vertical nitrate flux due to eddy pumping. *J. Geophys. Res.* **108**, doi:10.1029/2003JC001841 (2003).
10. Keeling, C. D., Brix, H. & Gruber, N. Seasonal and long-term dynamics of the upper ocean carbon cycle at Station ALOHA near Hawaii. *Glob. Biogeochem. Cycles* **18**, doi:10.1029/2004GB002227 (2004).
11. Karl, D. *et al.* The role of nitrogen fixation in biogeochemical cycling in the subtropical North Pacific Ocean. *Nature* **388**, 533–538 (1997).

12. Hannides, C. C. S. *et al.* Export stoichiometry and migrant-mediated flux of phosphorus in the North Pacific Subtropical Gyre. *Deep-Sea Res. II* **56**, 73–88 (2009).
13. Karl, D. M. *et al.* Ecological nitrogen-to-phosphorus stoichiometry at station ALOHA. *Deep-Sea Res. II* **48**, 1529–1566 (2001).
14. Ledwell, J. R., Watson, A. J. & Law, C. S. Evidence for slow mixing across the pycnocline from an open-ocean tracer-release experiment. *Nature* **364**, 701–703 (1993).
15. Church, M. J. *et al.* Physical forcing of nitrogen fixation and diazotroph community structure in the North Pacific subtropical gyre. *Glob. Biogeochem. Cycles* **23**, GB2020 (2009).
16. Behrenfeld, M. J. *et al.* Climate-driven trends in contemporary ocean productivity. *Nature* **444**, 752–755 (2006).
17. Emerson, S. & Hayward, T. L. Chemical tracers of biological processes in shallow waters of North Pacific: preformed nitrate distributions. *J. Mar. Res.* **53**, 499–513 (1995).
18. Anderson, L. A. On the hydrogen and oxygen content of marine phytoplankton. *Deep-Sea Res. I* **42**, 1675–1680 (1995).
19. Abell, J., Emerson, S. & Keil, R. G. Using preformed nitrate to infer decadal changes in DOM remineralization in the subtropical North Pacific. *Glob. Biogeochem. Cycles* **19**, GB1008 (2005).
20. Riser, S. C. & Johnson, K. S. Net production of oxygen in the subtropical ocean. *Nature* **451**, 323–325 (2008).
21. Letelier, R. M., Karl, D. M., Abbott, M. R. & Bidigare, R. R. Light driven seasonal patterns of chlorophyll and nitrate in the lower euphotic zone of the North Pacific Subtropical Gyre. *Limnol. Oceanogr.* **49**, 508–519 (2004).
22. Lamborg, C. H. *et al.* The flux of bio- and lithogenic material associated with sinking particles in the mesopelagic “twilight zone” of the northwest and North Central Pacific Ocean. *Deep-Sea Res.* **55**, 1540–1560 (2008).
23. Emerson, S., Stump, C. & Nicholson, D. Net biological oxygen production in the ocean: remote in situ measurements of O₂ and N₂ in surface waters. *Glob. Biogeochem. Cycles* **22**, doi:10.1029/2007GB003095 (2008).
24. McGillicuddy, D. J. Jr *et al.* Influence of mesoscale eddies on new production in the Sargasso Sea. *Nature* **394**, 263–266 (1988).
25. Karl, D. M. *et al.* in *Nitrogen in the Marine Environment* 2nd edn (eds Capone, D. G., Bronk, D. A., Mulholland, M. R. & Carpenter, E. J.) 705–769 (Elsevier, 2008).
26. Villareal, T. A. *et al.* Upward transport of oceanic nitrate by migrating diatom mats. *Nature* **397**, 423–425 (1999).
27. Johnson, K. S. & Coletti, L. J. In situ ultraviolet spectrophotometry for high resolution and long term monitoring of nitrate, bromide and bisulfide in the ocean. *Deep-Sea Res. I* **49**, 1291–1305 (2002).
28. Sakamoto, C. M., Johnson, K. S. & Coletti, L. J. An improved algorithm for the computation of nitrate concentrations in seawater using an in situ ultraviolet spectrophotometer. *Limnol. Oceanogr. Methods* **7**, 132–143 (2009).
29. Tengberg, A. *et al.* Evaluation of a lifetime-based optode to measure oxygen in aquatic systems. *Limnol. Oceanogr. Methods* **4**, 7–17 (2006).
30. Körtzinger, A., Schimanski, J. & Send, U. High quality oxygen measurements from profiling floats: a promising new technique. *J. Atmos. Ocean. Technol.* **22**, 302–308 (2005).

Supplementary Information is linked to the online version of the paper at www.nature.com/nature.

Acknowledgements This work was made possible by the engineering efforts of L. Coletti, H. Jannasch and D. Swift to integrate ISUS with the APEX float. C. Sakamoto performed ISUS sensor calibration. This work was supported by the David and Lucile Packard Foundation, the National Science Foundation, the National Oceanic and Atmospheric Administration and the US Office of Naval Research through the National Oceanographic Partnership Program. Funding was also provided by the Gordon and Betty Moore Foundation and the Center for Microbial Oceanography: Research and Education.

Author Contributions S.C.R. and K.S.J. wrote proposals to support incorporation of ISUS into the APEX float and co-lead the engineering effort to complete sensor integration. The system was deployed at the HOT station to take advantage of the background information and hypotheses generated by the HOT program, which was led by D.M.K. The initial data analysis was performed by K.S.J. and all authors contributed to writing the manuscript.

Author Information Reprints and permissions information is available at www.nature.com/reprints. The authors declare competing financial interests: details accompany the full-text HTML version of the paper at www.nature.com/nature. Readers are welcome to comment on the online version of this article at www.nature.com/nature. Correspondence and requests for materials should be addressed to K.S.J. (johnson@mbari.org).